

Paul M. Iñiguez\*

NOAA/National Weather Service, Phoenix, AZ

## 1. INTRODUCTION

### 1.1. Overview

It has long been hypothesized that urban areas exert a direct influence on precipitation patterns in their immediate surroundings (Horton, 1921). Early studies focused on this influence through the use of point-observation comparisons of urban and rural areas to quantify the anthropogenic effects on precipitation (AEP) (Changnon Jr., 1968, Huff and Changnon Jr., 1973, Huff and Schickedanz, 1974). Most, if not all, early studies suffered from inherent spatial and temporal errors due to the sampling methods used as they were unable to adequately measure convective precipitation (Lowry, 1998). Studies during the 1990s began to utilize higher resolution sampling techniques, which included lightning data (Westcott, 1995), satellite-based radar data (Shepherd et al., 2007), and ground-based radar data (Mote et al., 2007). Ground-based radar provides the most appropriate data for the study of AEP due to the superior spatial ( $1^\circ \times 1$  km) and temporal (approximately five minutes) resolution.

The study of AEP is important for several reasons:

- To quantify if and how human activities impact precipitation patterns, especially at the local scale.
- To understand possible changes to significant weather hazards (damaging winds, flash flooding, etc.) and how they impact society, including loss of property and/or life.
- To validate theoretical models which attempt to describe the causes of AEP.
- To serve as a proxy for larger scale studies on climate change with the results eventually incorporated into local and regional downscaling of global modeling efforts.
- To improve the accuracy of short-term forecasts of convective precipitation across urban areas.

---

\* *Corresponding author address:* Paul M Iñiguez, National Weather Service, PO Box 52025, Phoenix, AZ 85072; e-mail: paul.iniguez@noaa.gov

The Phoenix, AZ Metropolitan Area (PMA) represents a unique challenge in the study of AEP for several reasons, including significant variability in local topography (Fig. 2), an arid environment, and complicated convective processes. Two of three studies to date that focused on the PMA used flawed methodology, such as point-observational data (Diem and Brown, 2003) and satellite-based radar data with a resolution (spatial/temporal) far below that required to analyze convective precipitation (Shepherd, 2006). No previous study focused specifically on AEP across the PMA itself. The goal of this research was to determine if the urban areas of the PMA impact local summer-time precipitation patterns across the city.

### 1.2. Study Area

Spatially, the study area was defined by a  $1^\circ \times 1^\circ$  box centered on downtown Phoenix ( $33.444620^\circ$ ,  $-112.078400^\circ$ ), which encompasses nearly all areas typically associated with the PMA (Fig. 1). Temporally, precipitation data for the months of July and August were utilized, when the PMA is firmly under the influence of the North American Monsoon and precipitation is primarily convective and driven by a mixture of mountain/valley circulations and cold-pool interactions.

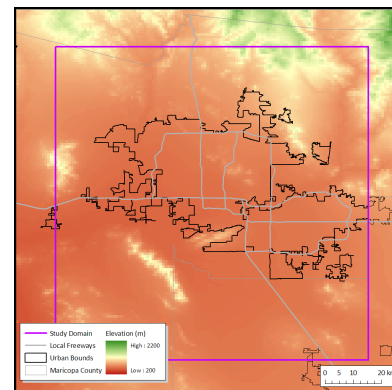


**Figure 1.** Study area (purple box), urban boundaries (black outlines), major freeways (gray lines), and topography (background image).

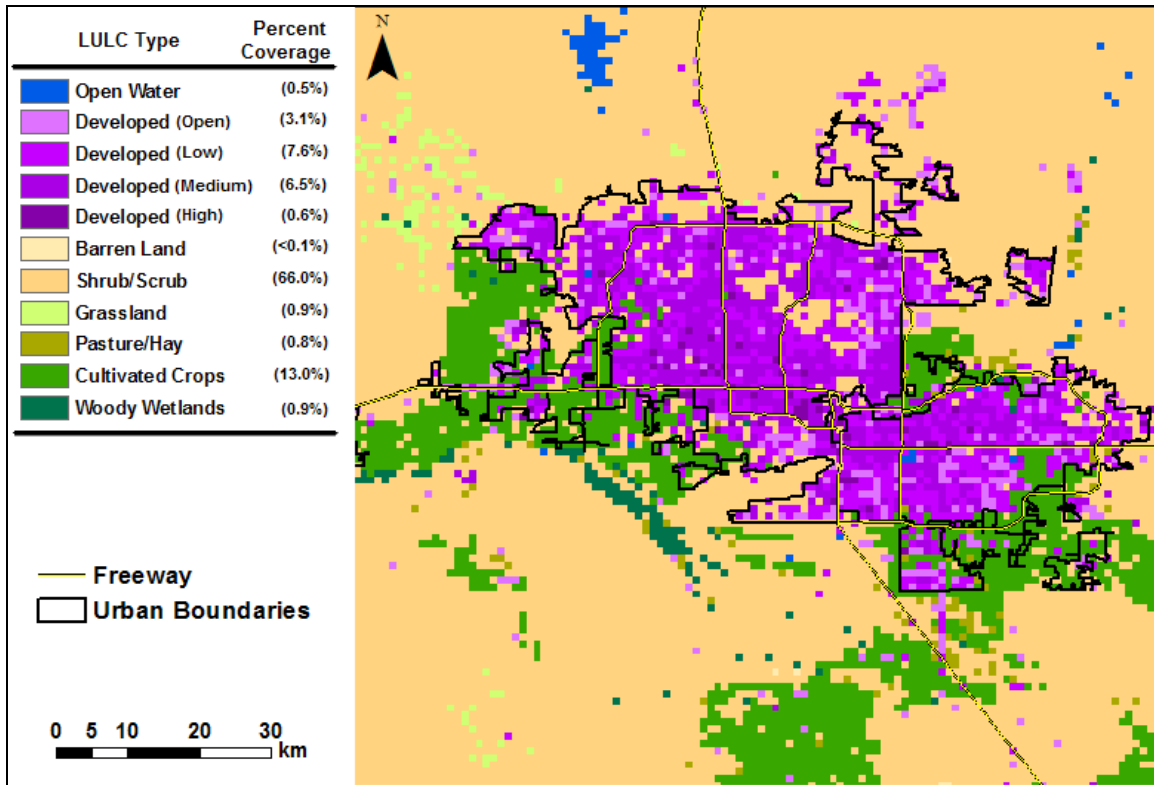


**Figure 2.** Land use/land cover type across the study domain. Purple areas represent developed areas (17.8% of total area).

## 2. DATA PREPERATION

### 2.1. Land Use/Land Cover Data

Land use/land cover (LULC) data from the National Land Cover Database (NLCD 2001), created by the Multi-Resolution Land Characteristic Consortium, were obtained from the U.S. Geological Survey Website ([www.mrlc.gov](http://www.mrlc.gov)). This dataset was developed from Landsat 5 and Landsat 7 satellite imagery by using decision tree software with training data, localized modelling, and hand-editing (Homer et al., 2007). The final product consisted of LULC classification (16 classes) for the entire United States at a 30m resolution. Data were obtained for the study domain, then up scaled from their native resolution of 30m to 1km using ESRI ArcMap (mode of smaller grids) in order to match the resolution of the precipitation dataset (Fig. 2). While this dataset is better utilized for regional and national studies, it is used here in order to provide a basis for possible comparative future studies of other metropolitan areas.

### 2.2. Radar Data

All one-hour precipitation (OHP) data available from the KIWA WSR-88D for the months of July and August were obtained free-of-charge through the NOAA National Climatic Data Center (NCDC) Web site (<http://www.ncdc.noaa.gov>). The months July and August were selected since convective precipitation is the predominant precipitation mode. The OHP product is generated roughly every five minutes (roughly twelve per hour). To reduce the amount of data used in this study, OHP files nearest to the top of each hour were retained while the rest were discarded. This resulted in a database of OHP roughly on the hour, for each hour, from 01Z 1 July through 23Z 31 August.

An analysis of data completeness revealed that a severe lack of data existed from 1994 through 2000 due to periodic equipment failures. Therefore, only data from the years 2001 through 2008 were used in this study. Software made available by the NOAA NCDC was utilized to convert the OHP files from their native unique digital binary format in polarimetric coordinates (resolution 1x1km) to the Arc/Info ASCII Grid (ASC) format (resolution 1km x 1km).

## 2.3. Radar Data Quality Control

### 2.3.1. Ground Clutter

A potential source of error for OHP is ground clutter, a significant concern within the study area due to the existence of several small mountain ranges (White Tank Mountains, Estrella Mountains, South Mountain, San Tan Mountains, McDowell Mountains, and Phoenix Mountains) and several central business districts with buildings encroaching on a height of 150m. When atmospheric conditions become conducive to superrefraction, the previously mentioned ground features are erroneously detected and measured as precipitation by the radar. While many quality control features reduce the effects of ground clutter, a strong positive bias in the OHP product exists as a consequence of residual unfiltered ground clutter.

In order to identify grid points impacted by ground clutter, the number of hours (frequency) of precipitation at each grid point was tallied through the entire dataset (2001-2008). A histogram of total hours of precipitation at each grid point indicates a Poisson distribution with a mean and standard deviation of 120 hours. From the histogram, it is clear that grid points with observed precipitation frequency greater than one standard deviation from the mean, or greater than 240 hours, are outliers. A spatial display of the frequency data confirms the outlier grids are near elevated locations, central business districts, or the radar itself (Fig. 3). A mask containing the x,y coordinates of the outlier grid points was generated then employed in further analysis.

### 2.3.2. RDP Accuracy

To assess the accuracy of the radar data, the radar-derived precipitation data (RDP) were compared to gage-measured precipitation data (GMP) from a dense network of rain gages situated across the PMA. This 300-plus rain gage network is operated by the Flood Control District of Maricopa County (FCD). This secondary dataset is made available by the FCD through their Web site (<http://www.fcd.maricopa.gov>). Gage selection was based on the following criteria: the gage was installed prior to 1 July 2001, was within the study domain, and was not located in a masked radar grid box. An analysis of gage metadata revealed that of 305 gages, 133 met the outlined criteria (Fig. 3).

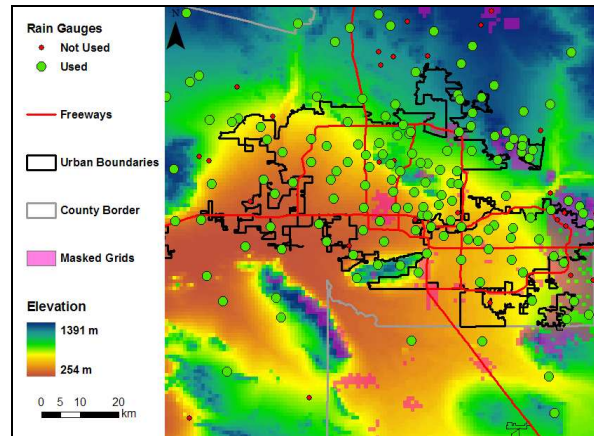


**Figure 3.** Topographic map of the study domain. Green (red) dots indicate the location of rain gauges used (not used) in a RDP-GMP comparative analysis. Masked grids are also indicated (purple shading).

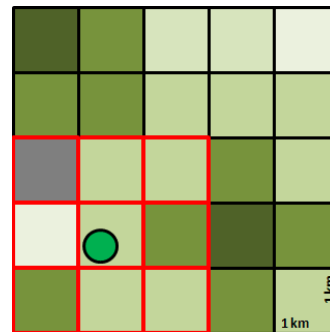


**Figure 4.** Graphical demonstration of the process used to determine RDP. This sample 5x5 grid represents precipitation (increasing from light to dark green). The green dot represents the location of a rain gage. The 3x3 sub-grid (highlighted red) centered on the rain gage is used to determine an average RDP. Note that one of the sub-grids is gray indicating it has been masked in the calculation.

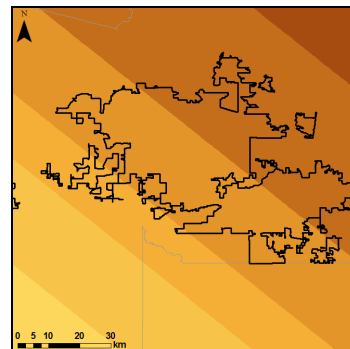


**Figure 5.** First-order surface trend analysis of average seasonal precipitation indicating relative gradient decreasing from NE to SW. Urban areas outlined in black.

The two unique precipitation datasets, RDP and GMP, were aggregated into seasonal totals, from 2001 through 2008. The aggregation of data was simple and straight-forward for the GMP and only required addition of the base data. A more involved process was required for the RDP. Ideally, each gage would have a corresponding (x,y) grid point in the radar grid field for which RDP could be aggregated. However, since the radar typically measures “rain” at a location well above the ground (several hundred to several thousand feet), factors such as wind below the radar beam and rain/cloud movement could cause the rain to fall into adjoining grid points. To account for this slight advective uncertainty, the average RDP of a 3x3 sub-grid centered on the (x,y) grid point where each gage was located was calculated for all 133 rain gage locations (Fig. 4). In the event that part of the 3x3 sub-grid fell into a masked area, the masked portion of the sub-grid was ignored. These processes resulted in eight new datasets, one for each season, comprised of two columns (RDP and GMP) and 133 rows (one row per gage/sub-grid pair).

Descriptive statistics for the GMP and RDP were computed using the Minitab software. Based on standard statistical significance tests of skewness, kurtosis, and the Kolmogorov-Smirnov, it was found that many of the datasets were significantly positively skewed and/or leptokurtic. To reduce/remove detected non-normalities, a square root transformation was applied to all GMP and RDP. While some of the post-transformation datasets still indicated a deviation from normality, based on probability plots and histograms it was determined that the distributions approached normality and were skewed by only a small handful of outliers. A statistically significant deviation from normality in the kurtosis statistic is considered reasonable given the relatively small study area.

A linear regression analysis between the transformed GMP (predictor) and RDP (predictand) was completed using the Minitab software for each year in the comparative dataset. In all seasons, a statistically significant correlation existed between the GMP and RDP, with adjusted  $r^2$  ranging from 29.6% to 64.8%. Based on the slope from the linear regression equation(s), on average, the radar over-estimated actual precipitation by a factor of 1.6 (min: 1.3, max: 2.4). Scatterplots of the regression analysis confirm the linear trends. It is concluded that the RDP are

comparatively accurate and suitable for further analyses.

### 2.3.3. Detrending

A first-order surface trend analysis of average seasonal precipitation data revealed a significant gradient in the dataset, with higher amounts to the northeast (Fig. 5). For this analysis, each row and column was de-trended to remove this bias for each season (2001-2008). To do this, the difference between modeled precipitation and measured precipitation was computed for each grid point using equation 1.

$$y'_i = y_i - (m \times x_i + b) + \bar{y} \quad (1)$$

where  $y'_i$  is the de-trended precipitation amount for the  $i^{\text{th}}$  element of the row (column);  $y_i$  is the observed precipitation for the  $i^{\text{th}}$  element of the row (column);  $(m \times x_i + b)$  is the modeled precipitation amount for the  $i^{\text{th}}$  element of the row (column) with the predictor ( $x_i$ ) simply the row (column) number,  $m$  the slope of the linear regression line for the row (column), and  $b$  the intercept;  $\bar{y}$  is the average precipitation for the row (column). Any masked grid point was not used in the de-trending process. A similar technique was done for precipitation frequency.

## 3. RESULTS

### 3.1. LULC Impacts on Precipitation

Using the de-trended seasonal RDP and LULC type data, the average seasonal precipitation and average seasonal frequency of precipitation was determined by LULC type (Table 1). The data indicate LULC type by itself does not impact convective precipitation at the seasonal scale, either by amount or frequency.

### 3.2. Spatial Trends

A second-order surface trend analysis of the average seasonal precipitation revealed a precipitation deficit over the center of the study domain (Fig. 6). Therefore, when larger trends are accounted for, on average it rains less (approximately 15%) of the center of the study domain as compared to the outer edges of the study domain. Without the removal of the northeast to southwest precipitation gradient, this result would likely not have been found (Fig. 7).

**Table 1.** Precipitation amounts and frequencies by LULC type as determined by quality-controlled radar-derived precipitation across the Phoenix, AZ Metropolitan Area. No LULC type significantly deviates from the others.

LULC Type	Seasonal Precipitation (inches)		Precipitation Frequency (hours)	
	Average	Standard Deviation	Average	Standard Deviation
Open Water	2.89	1.21	10.95	4.13
Developed, Open Space	2.48	0.89	9.84	3.90
Developed, Low Intensity	2.39	0.94	9.38	3.83
Developed, Medium Intensity	2.40	0.93	9.48	3.94
Developed, High Intensity	2.73	1.32	10.75	5.53
Barren Land	2.37	0.63	11.03	3.56
Shrub/Scrub	2.71	0.77	10.60	3.49
Grassland	2.68	0.73	10.03	3.37
Pasture/Hay	2.56	0.74	9.85	3.23
Cultivated Crops	2.49	0.74	10.25	3.93
Woody Wetlands	2.51	1.09	9.47	4.06

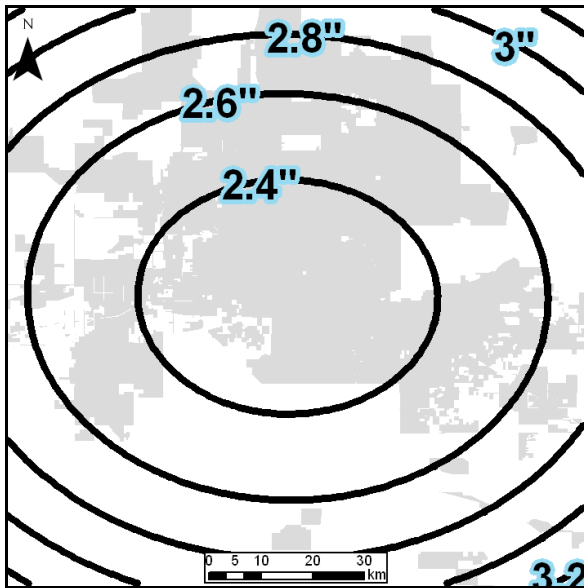


**Figure 6.** Second-order surface trend analysis of average seasonal precipitation overlaid on urban areas (shaded in gray).

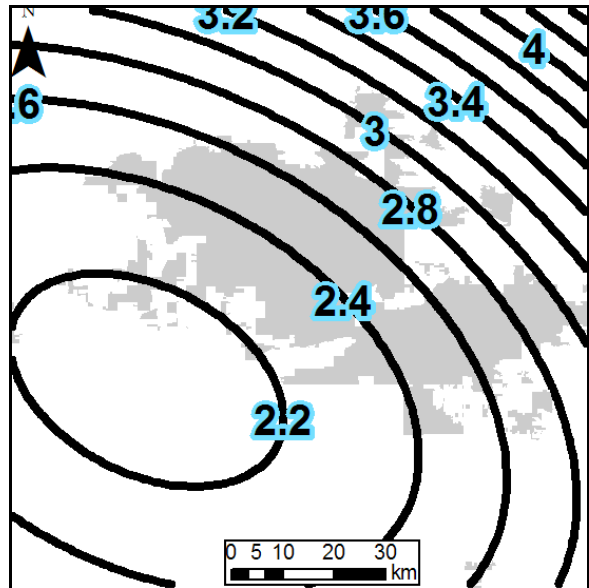


**Figure 7.** Second-order surface trend analysis of RDP without trend removed overlaid on urban areas (shaded in gray).

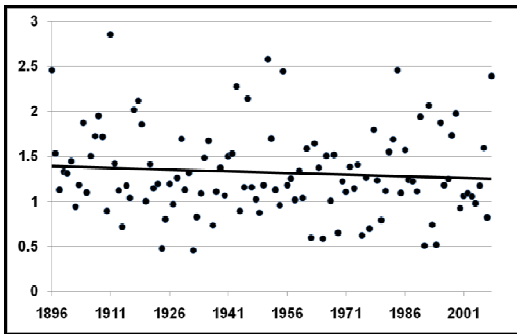


**Figure 8.** Plot of July-August precipitation by year (1896-2008) as measured in Phoenix, AZ. A square root transformation has been applied to the data. Linear regression analysis indicates that precipitation has decreased at a rate of 0.16 inches century<sup>-1</sup>.

#### 4. CONCLUSION

This paper represents the most exhaustive study to date on precipitation patterns across the PMA. The results are bolstered by the use of radar-derived precipitation data, which have the necessary spatial and temporal resolution to study convective precipitation. These data were made even more robust through cautious quality control methods which greatly reduced errors common to RDP (ground clutter). A thorough comparison of RDP to GMP further strengthened the case of utilizing RDP in this study.

The fact that there was no detectable impact of LULC type on precipitation amounts and frequencies, yet a larger precipitation deficit anomaly was found, suggests that only when taken as a whole does the PMA impact convective precipitation. However, it may not be reasonable to make this connection as it is entirely possible that the deficit is naturally occurring with or without the existence of the PMA. If the urban areas were driving this precipitation deficit, it would be reasonable to assume this deficit manifested itself over time as the PMA grew. A plot of long-term precipitation measured in Phoenix, AZ shows that precipitation has decreased at a rate of 0.16 inches century<sup>-1</sup> (Fig. 8). This equates to a decrease of approximately 0.2 inches since 1900, roughly half the deficit found in Figure 6, thus suggesting the PMA is partly responsible.

To the common observer, this reduction in precipitation is likely not detectable, as it was only found through mathematical manipulation of the data (second order surface trend analysis of de-trended data).

#### REFERENCES

- Changnon Jr., S. A., 1968. The La Porte weather anomaly – fact or fiction? *Bull. Am. Meteorol. Soc.*, **49**, 4-11.
- Diem, J. E., and Brown, D. P., 2003: Anthropogenic Impacts on Summer Precipitation in Central Arizona, U.S.A. *The Professional Geographer*, **55**, 343-355.
- Homer, C., J. Dewitz, J. Fry, M. Coan, N. Hossain, C. Larson, N. Herold, A. McKerrow, J.N. VanDriel and J. Wickham. 2007: Completion of the 2001 National Land Cover Database for the Conterminous United States. *Photogrammetric Engineering and Remote Sensing*, **73:4**, 337-341.
- Horton, R. E., 1921: Thunderstorm-Breeding Spots. *Monthly Weather Review*, **49**, 193.
- Huff, F. A., and Changnon Jr., S. A., 1973: Precipitation modification by major urban areas. *Bull. Am. Meteorol. Soc.*, **54**, 1220-1232.
- \_\_\_\_\_, and Schickedanz, P. T., 1974: METROMEX: Rainfall Analysis. *Bull. Am. Meteorol. Soc.*, **55**, 90-92.
- Lowry, W. P., 1998: Urban effects on precipitation amount. *Progress in Physical Geography*, **22(4)**, 477-520.
- Mote, T. L., Lacke, M. C., and Shepherd, J. M., 2007: Radar signatures of the urban effect on precipitation distribution: A case study for Atlanta, Georgia. *Geophys. Res. Lett.*, **34**, 1-4.
- Shepherd, J. M., Pierce, H., and Negri, A. J., 2002: Rainfall Modification by Major Urban Areas: Observations from Spaceborne Rain Radar on the TRMM Satellite. *J. Appl. Meteorol.*, **41**, 689-701.
- Shepherd, J. M., 2006: Evidence of urban-induced precipitation variability in arid climate regimes. *Journal of Arid Environments*, **67**, 607-628.
- Westcott, N. E., 1995: Summertime Cloud-to-Ground Lightning Activity around Major Midwestern Urban Areas. *J. Appl. Meteorol.*, **34**, 1633-1642.